Proc. Schl. Eng. Tokai Univ., Ser. E
36 (2011) 79-87

Evaluations and Improvement of Ride Comfort Performance of Electric Vehicle Conversion

Saiful Anuar ABU BAKAR*1, Ryosuke MASUDA*2, Hiromu HASHIMOTO*3,
Takeshi INABA*4, Hishamuddin JAMALUDDIN*5, Roslan ABD. RAHMAN*5,
Pakharuddin MOHD. SAMIN*6.

(Received on Aug. 4 and accepted on Sept. 20, 2011)

Abstract

This paper present a study on ride comfort performance of passenger vehicle converted into an electric vehicle. The studies involved evaluations on the vehicle's ride comfort performance before and after the conversion, as well as possible ride comfort performance improvements by the magnetorheological semi active suspension system. The studies used 7 degrees of freedom of vehicle's ride model which were validated experimentally. The data of Malaysian made passenger vehicle were used in this study assuming that the vehicle is going to be converted into an electric vehicle. Ride test known as pitch mode tests were conducted to validate the reliability of the developed simulation model. The validated simulation model was used to evaluate the vehicle ride comfort performance when converted into an electric vehicle. The validated simulation model was also integrated with the semi active suspension system in order to improve the EV conversion ride comfort performance. It was found that the EV conversion's ride comfort was not significantly affected from the modifications and the application of semi active suspension system can be an alternative in further improving the EV conversion's ride comfort performance.

Keywords*: electric vehicle conversion, ride comfort, semi active suspension system, magnetorheological*

Introduction

The development of electric vehicle (EV) from the commercially available vehicle model is becoming a trend nowadays due to the global concerns in reducing the green house effect which one of its contributing factors came from the pollution of vehicle. An electric vehicle that is being converted from a normal production vehicle model usually known as a electric vehicle conversion or EV conversion.

Electric vehicle is driven by electric motor. It is either uses only two or four electric motors to move the vehicle. Other common component that can be seen in an electric conversion vehicle are batteries, AC/DC or DC/DC converters, battery management system, pedal relays and others auxiliary components such as electric power steering. Many research works were found to focus on the electric vehicle's electric and electronic systems but not many were found to focus in improving EV conversion's stability while manoeuvrings. The researches on EV conversion's stability are mainly related to the yaw stability control and traction system.

In yaw stability control on electric vehicle [1~4] it focuses in controlling yaw motion of the electric vehicle by controlling the operation of the drive motor.

*1 Graduate Student, Course of Science and Tehcnology, Graduate School of Science and Technology
*2 Professor, Department of Applied Computer Engineering
*3 Professor, Department of Mechanical Engineering
*4 Associate Professor, Department of Applied Computer Engineering
*5 Professor, Department of Applied Engineering, UTM
*6 Associate Professor, Department of Automotive Engineering, UTM

The drive motor, either two or four are basically controlled in terms of its torque generation. While in traction control system [5~7] the generation of electric motor torque is controlled to ensure the wheel does not skid while accelerating ensuring full control over the vehicle. This is done by controlling the slip ratio of the wheel.

It is not clear how the modifications towards an EV conversion affect the vehicle's ride comfort performance; the level of isolations of passenger compartment from being affected by harsh road profile. Typically, any conversion of internal combustion engine vehicle to electric vehicle involves some weight addition (or weight reduction). This is due to the installations of the electric vehicle systems i.e. battery system and converters. Any weight addition or weight reduction on the chassis will cause the vehicle's weight distribution to change and this compromised the vehicle's ride comfort performance, as current suspension system tuning was not being designed specifically for the new weight and load distribution at front and rear axles. This paper will investigate the affects of weight distribution changes on EV conversion's ride comfort performance and possible improvement of EV conversion's ride comfort performance using magnetorheological semi active suspension system.

2. Mathematical Modelling of Ride Comfort Model

A vehicle's ride model is derived based on the work done in [8]. The ride model consists of seven degrees of freedom namely roll, pitch, bounce and vertical motion of each four wheels. Figure 1 show the vehicle' ride model.

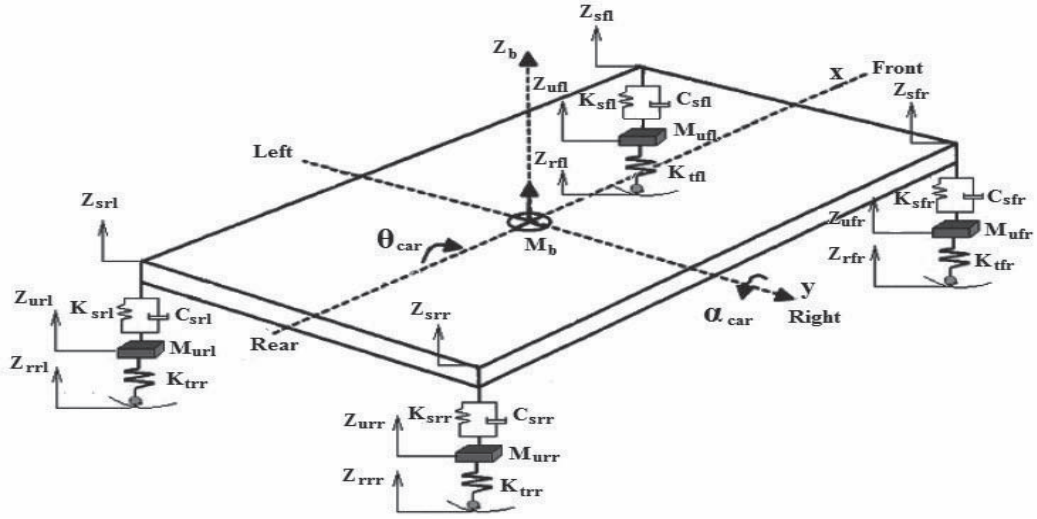

Fig. 1 Seven degree of freedom of vehicle ride model

Based on the 7DOF of ride model in Figures 1, the displacements of the sprung masses are given by;

$$Z_{sij} = Z_b + \frac{a_{car}}{2}\theta_{car} - L_i\alpha_{car} \quad (1)$$

with Z_{sij} is the total sprung mass displacement (i =*f* for front, *r* for rear and *j*=*l* for *le*ft, *r* for right), Z_b is the sprung mass vertical displacement at the center of gravity, θ_{car} is the roll angle and α_{car} is the pitch angle. The distance of centre of gravity to the front axle and rear axle are given by L_f and L_r respectively. The forces acting at each of the suspension (F_{ij}) is the sum of the spring force (F_{sij}) and damper force (F_{dij}). The suspension forces are given by

$$F_{ij} = F_{sij} + F_{dij} \quad (2)$$

The spring forces, F_{sij} in each of the suspension system are given by;

$$F_{sij} = K_{sij}(Z_{uij} - Z_{sij}) \quad (3)$$

with K_{sij} is the spring stiffness of the spring, Z_{uij} and Z_{sij} are the unsprung mass vertical displacement and the sprung mass vertical displacement respectively at each side of the vehicle. The damper forces, F_{dij} are given by;

$$F_{dij} = C_{sij}(\dot{Z}_{uij} - \dot{Z}_{sij}) \quad (4)$$

with C_{sij} are the damping coefficient of the dampers, $\dot{Z}_{uij}$ and $\dot{Z}_{sij}$ are the unsprung mass vertical velocity and the sprung mass vertical velocity respectively. For the vehicle tires, it is modelled as a spring and the force acting at tires is usually known as dynamic tire loads, F_{tij}. For each tires, their dynamic tire loads are given by;

$$F_{tij} = K_{tij}(Z_{rij} - Z_{uij}) \quad (5)$$

where K_{tij}, Z_{rij}, and Z_{uij}, are the tire stiffness, road input displacement and unsprung mass displacement respectively.

Using Newton's Second Law at the vehicle's sprung mass, the body vertical acceleration, $\ddot{Z}_b$ can be determined by

$$F_{fl} + F_{fr} + F_{rl} + F_{rr} = M_b\ddot{Z}_b \quad (6)$$

where M_b is the total mass of the vehicle. Angular acceleration during the roll effect, $\ddot{\theta}_{car}$ is given by;

$$(F_{fl} + F_{rl})\frac{a_{car}}{2} - (F_{fr} + F_{rr})\frac{a_{car}}{2} = I_{xx}\ddot{\theta}_{car} \quad (7)$$

where a is the vehicle's track width and I_{xx} is the moment of inertia about *x*-axis. The angular acceleration while the vehicle is in pitch effect, $\ddot{\alpha}_{car}$ it is given by;

$$(F_{rl} + F_{rr})L_r - (F_{fl} + F_{fr})L_f = I_{yy}\ddot{\alpha}_{car} \quad (8)$$

with I_{yy} are the vehicle's wheelbase and moment about *y*-axis respectively. Acceleration of each wheel can be calculated using

$$F_{tij} - F_{sij} - F_{dij} = M_{uij}\ddot{Z}_{uij} \quad (9)$$

with M_{uij} are the unsprung masses at each corner of the vehicle. The vehicle ride comfort model was developed using equations (1) to (9) using Matlab/Simulink.

3. VALIDATION OF VEHICLE RIDE MODEL

The developed vehicle ride model was validated with an experimental vehicle in order to determine the model's reliability in representing an actual vehicle's ride behaviours. A Malaysian made vehicle was used in validating the developed simulation model.

In vehicle's instrumentation preparations, several types of transducers were used and there are three-axis sensor that measure vertical, longitudinal and lateral acceleration as well as the rotational motions (roll, pitch and yaw). The three-axis sensor was located approximately at the centre of gravity of the vehicle. An amount of 8 units of single axis accelerometer were installed at each corner of the vehicle, at the sprung and unsprung masses. The accelerometers were used to measure vertical acceleration of vehicle's sprung and unsprung masses when the vehicle hit the bump. A multi-channel Dewetron data acquisition system was used for the data collection. Figure 2 shows the instrumentation setup in the vehicle.

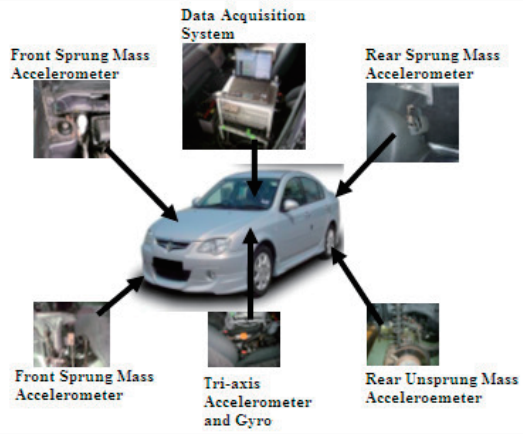

Fig. 2 Instrument setup in experimental vehicle

A pitch test was performed during the experiment. In pitch test, a bump with the dimensions of 2.4m in length, 0.4m in width and 0.075m in height, was used and arranged perpendicularly to the vehicle's driving direction. A speed of 20km/h was used during this test. In this pitch test, the front wheels will hit the bump followed by the rear wheels.

Table 1 shows the vehicle parameters used for the simulation model and Figure 3 shows the validation results between the experimental and simulation data. It can be seen that there is a good correlations between the simulation and experimental data; in terms of responses' trends.

4. RIDE COMFORT EVALUATIONS ON EV CONVERSION

The validated ride model was later used to study the effect of modifications on the passenger vehicle into an electric vehicle. It is assumed that the experimental vehicle is about to be converted into an electric vehicle. The effects of weight distribution in electric vehicle conversion (EVC) which is biased to the rear of the vehicle, due to the battery system are investigated. The evaluations were done by considering two weight distribution ratios; 60:40 and 40:60 weight distribution ratios. The 60:40 weight distribution ratio is the assumption of weight distribution before modifications while 40:60 weight distribution ratio is the assumption ratio, after modifications is done. The weight distribution used, determined the position of centre of gravity from front and rear axles, L_f and L_r respectively. Below are the relation between weight distribution and the distance of CG to front and rear axles:

$$W_f = \frac{W_t}{L} L_r \quad (10)$$

$$W_r = \frac{W_t}{L} L_f \quad (11)$$

where W_f , W_r and W_t are weight at the front axle, weight at the rear axle and vehicle total weight respectively. Vehicle parameter data in Table 1 were used in evaluating the ride comfort of the vehicle, before and after the conversions.

5. EV CONVERSION WITH SEMI ACTIVE SUSPENSION SYSTEM

Semi active suspension system is considered in improving EV conversion's ride comfort performance. Semi active suspension system is a suspension consists of conventional spring and a variable damping damper, controlled electronically. The variable damping damper can be either a variable orifice damper or a damper which uses smart material such as Magnetorheological (MR) damper.

Table 1 Vehicle Parameters

Mb	1250 kg	Ksfl	17900 N/m
Mufl	50 kg	Ksfr	17900 N/m
Mufr	50 kg	Ksrl	17900 N/m
Murl	50kg	Ksrr	17900 N/m
Murr	50 kg	Csfl	3100 Ns/m
a	1.5	Csfr	3100 Ns/m
L	2.6	Csrl	3100 Ns/m
Ixx	289 kgm^2	Csrr	3100 Ns/m
Iyy	3300 kgm^2	Lf (60:40)	1.56 m
Izz	13350	Lr (60:40)	1.04 m
Iw	0.87 kgm^2	Lf (40:60)	1.04 m
Re	0.287 m	Lr (40 :60)	1.56 m
c	0.469 m		
Ktfl	23000 N/m		
Ktfr	23000 N/m		
Ktrl	23000 N/m		
Ktrr	23000 N/m		

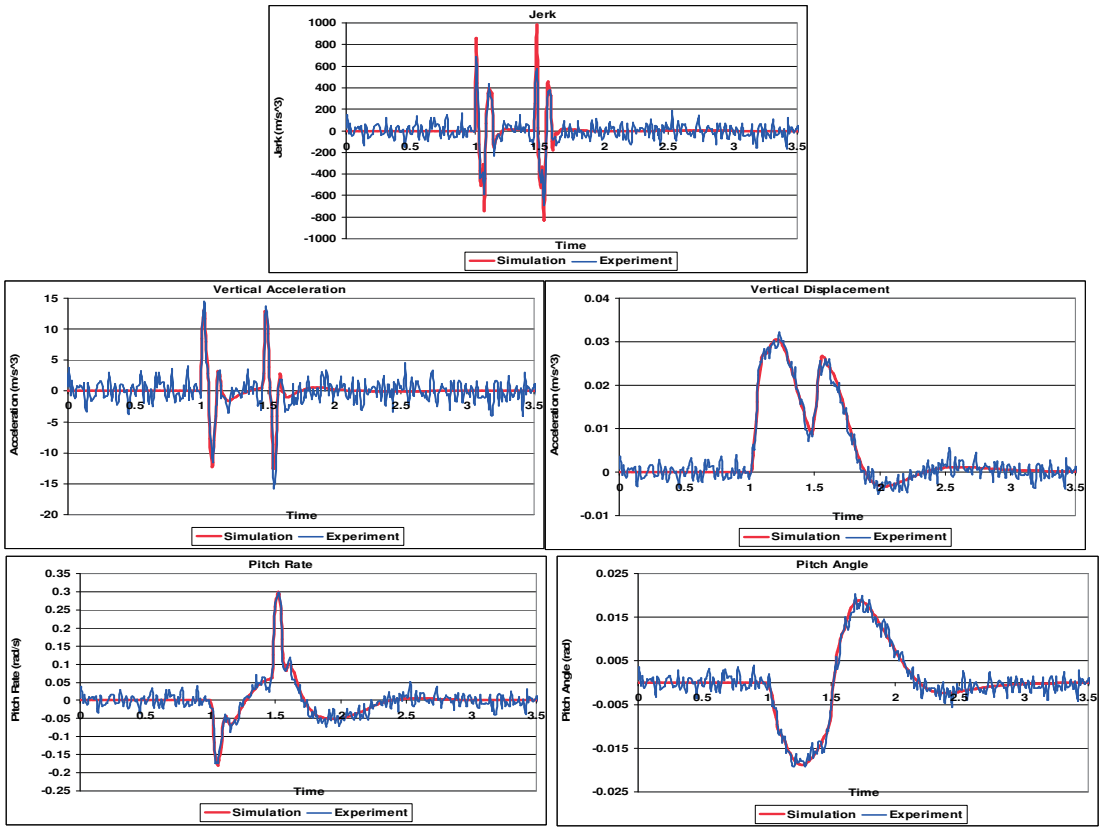

Fig. 3 Validations between simulation and experimental data during pitch test

5.1 Modelling of Magnetorheological and Current Generator Model

The Magnetorheological (MR) damper was used as a damping element in EV conversion's semi active suspension system. Figure 4 shows the characteristic a Delphi Magneride Magnetorheological damper used in this study.

The characteristics of the MR damper was modelled using the non-parametric data mapping approach [10]. Based on Figure 4, the data mapping involves the mapping of damping force data from 0 to 5 Ampere with the velocities range is ±1 m/s. A linear interpolation and extrapolation on a force-velocity curve will be made when the input velocity value to the MR damper is outside or located between the velocity data using linear interpolation-extrapolation equations.

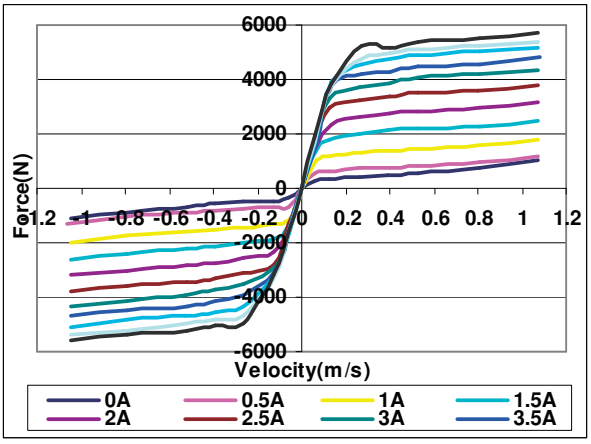

Fig. 4 Delphi MR damper characteristic [9]

The current generator model [10] was developed based on the inverse characteristic of the Delphi MR damper's characteristic. The current generator model is used to generate specific amount of current based on the relative

5.2 Skyhook Control Algorithm

Skyhook control system [1] is the most basic and most common algorithm used in semi-active suspension system for disturbance rejection control. In skyhook control system (Figure 5), an imaginary damper is inserted between the sprung mass and the stationary sky as shown in Figure 5, as an effort to reduce or eliminate the motions of sprung mass when the vehicle is subjected to road inputs such as road harshness or bumps.

In essence, the skyhook configuration adds more damping to the sprung mass and takes away damping from the unsprung mass. The skyhook configuration is ideal if the primary goal is to isolate the sprung mass from base excitations, even at the expense of excessive unsprung mass motion.

The control policy of skyhook system can be summarized as follows: if the product of the sprung

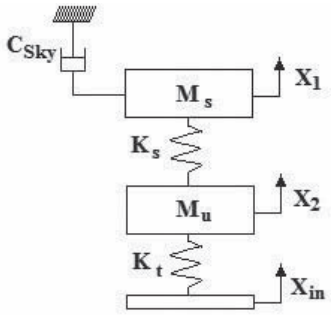

Fig. 5 Skyhook system

mass velocity, X_1 and relative velocity between the sprung mass and unsprung masses, X_{12} is positive, the semi-active force is proportional to the velocity of sprung mass. Else, the semi-active damping force is set to zero. The equation governing skyhook control is given by:

$$\text{If } \dot{Z}_s(\dot{Z}_u - \dot{Z}_s) \geq 0 \text{ then } F_d = C_{high}(\dot{Z}_u - \dot{Z}_s)$$

$$\text{If } \dot{Z}_s(\dot{Z}_u - \dot{Z}_s) < 0 \text{ then } F_d = C_{low}(\dot{Z}_u - \dot{Z}_s) \quad (12)$$

where, C_{high} and C_{low} is the damping coefficient constants while $\dot{Z}_u$ and $\dot{Z}_s$ is the unsprung mass velocity and sprung mass velocity respectively. In the original skyhook algorithm, C_{low} is chosen to be 0 because ideally the suspension need to provide maximum force absorption without any damping resistance. However this is impossible because the damper will always have a minimum damping force due to the fluid friction.

In this simulation the value of C_{low} was chosen to be at 1000 Ns/m while the value for C_{high} was tuned towards an optimal ride comfort performance. The value for C_{low} was chosen based on a random selections within the range of 500 to 1000 Ns/m. It was found that the value of 1100 Ns/m for C_{high} gave an optimum overall improvement (Figure 6) and at the same time is causing minimum current consumption required by the MR damper to operate (Figure 7). It also gave minimum error in terms of force tracking between the estimated damping force from the controller and the actual damping force produced by the Magnetoheological damper (Figure 8).

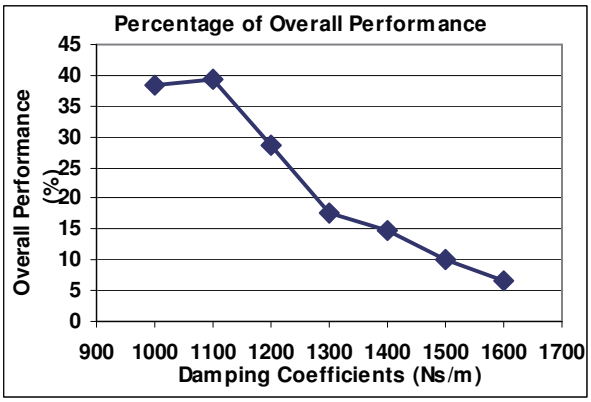

Fig. 6 Optimization for maximum overall performance

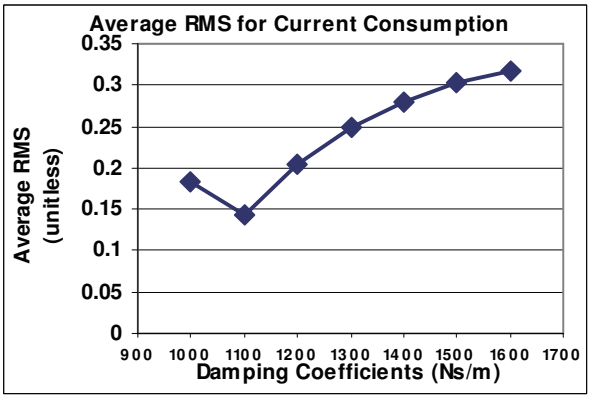

Fig. 7 Optimization for minimum current consumption

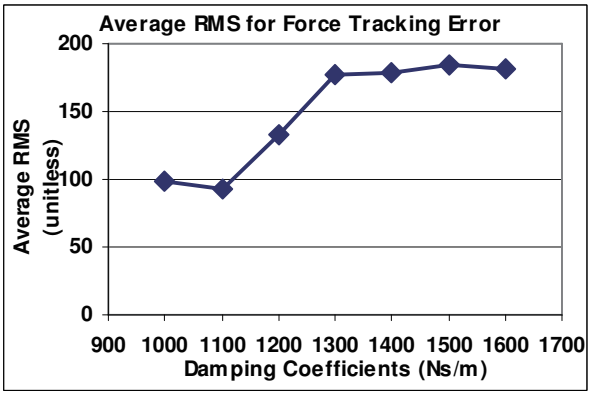

Fig. 8 Optimization for minimum error in force tracking by MR damper

6. SIMULATION RESULTS

The EV conversion's ride model is evaluated using the pitch test. In pitch test, the simulation model is subjected to a road profile (bump arrangement), which will create pitching motion on the vehicle. The bump input was arranged perpendicular to the direction of EV conversion's travel.

The vehicle model was simulated to move at a constant speed of 20 km/h before hitting a bump input with the height, width and length of 0.075m, 0.4m and 2.44m respectively. The simulation time used to run the simulation model is 3.5 s. The speed was chosen to be the same as the experimental validation, mentioned previously in Section 3 in order to evaluate the effectiveness of the studied semi active suspension system if installed on the EV conversion vehicle and drove at the same experimental speed.

Table 2 shows the RMS values of the studied responses on the vehicle before the conversion, after the conversion and the EV conversion's responses with the semi active suspension system. While Figure 9 shows the results of the studied responses in time domain form. The frequency response of the vehicle before and after conversion can be referred to Figure 10.

Based on Table 2 and Figure 9, it can be seen that the changes of weight distributions due to the modifications towards an electric vehicle did not affects the EV conversion's ride comfort significantly. However it is observed that the changes of weight distribution did effects vehicle's vertical displacement when the rear wheel hit the bump; 40:60 weight distribution model is having a higher vertical displacement compared to the 60:40 weight distribution model. The implementation of semi active suspension system in the EV conversion improves significantly the EV conversion ride comfort by almost 40 percents where the most significant improvements can be seen were made in terms of EV conversion's vertical displacement and pitch angle. In terms of frequency response of the EV conversion (Figure 10), the major frequency response for the EV conversion remained the same as before the modifications were done which is at 1.583 Hz. However the frequency response for the EV conversion with the semi active suspension system is slightly increased to 1.636 Hz. Even though the value is slightly higher, the frequency response value for the EV conversion with the semi active suspension system is however compromised due to the fact that the semi active suspension system is improving the studied responses in terms of its magnitudes.

Another aspects studied in this paper are the amount of current consumption used by the MR damper model to operate as well the MR damper model abilities to execute the estimated damping force from the controller (the skyhook algorithm). Figure 11 shows the amount of current supplied to the MR damper during the pitch simulation test. It can be seen that the operation of the damper requires low current consumption in order to operate which is no more than 1.5 Amperes. This is due to the executable estimated damping force from the controller by the MR damper. If the estimated damping force from the controller is beyond the capability of the MR damper to produce, maximum current will always be supplied to the MR damper so that the MR damper will produce the damping force as high as possible; approximately to the beyond-executable damping force estimated by the controller. In terms of force tracking ability by the MR damper model with the estimated damping force from the controller (Figure 12), it can be seen that the MR damper model is able to produce the damping force approximately the same as estimated by the controller. It is important to ensure that the actual

damping force produced by the MR damper is approximately the same as the estimated damping force to ensure the semi active suspension system is giving an optimal ride comfort performance without causing the semi active suspension system to 'under-work' or 'over-work'. This is done by optimally tune the controller used in this type of suspension system.

7. CONCLUSIONS

As for conclusions, the vehicle modifications into an electric vehicle do not significantly reduce the vehicle ride comfort performance except the vehicle's vertical displacement response. This is possibly being improved by using the magnetorheological semi active suspension system. In this study, the semi active suspension system was found not only to improve the EV conversion's vertical displacement response, but other responses as well i.e. jerk, vertical acceleration, pitch rate and pitch angle. Low current consumption in operating the magnetorheological damper in the EV conversion has also made the semi active suspension system, a good alternative of suspension system to be incorporated in real world EV conversion, since it does not add significant electrical load to the power system of the EV conversion.

REFERENCES

[1] Shino, M., Miyamoto, N., Wang, Y. Q. and Nagai, M. (2000). Traction Control of Electric Vehicles Considering Vehicle Stability. *Advanced Motion Control, 2000. Proceedings. 6th International Workshop on Advanced Motion Control.*

[2] Niasar, A. H., Moghbeli, H. and Kazemi, R. (2003). Yaw Moment Control Via Emotional Adaptive Neuro-Fuzzy Controller for Independent Rear Wheel Drives of an Electric Vehicle. *Proceedings of 2003 IEEE Conference on Control Applications.*

[3] Donghyun, K., Sungho, H. and Hyunsoo, K. (2005) Rear Motor Control for a 4wd Hybrid Electric Vehicle Stability. *IEEE International Conference on Vehicular Electronics and Safety*

[4] Miyazaki, H. and Ohmae, T. (2005). Driving Stability for Electric Vehicle with Independently Driven Two Wheels in Case of Inverter Failure. *European Conference on Power Electronics and Application.*

[5] Sado, H., Sakai, S. and Hori, Y. (1999). Road Condition Estimation for Traction Control in Electric Vehicle. *Proceedings of the IEEE International Symposium on Industrial Electronics.*

[6] Pusca, R., Ait-Amirat, Y., Berthon, A. and Kauffmann, J. M. (2002). Modeling and Simulation of a Traction Control Algorithm for an Electric Vehicle with Four Separate Wheel Drives. *IEEE 56th Vehicular Technology Conference.*

[7] Wjalili-Kharaajoo, M. and Besharati, F. (2003). Sliding Mode Traction Control of an Electric Vehicle with Four Separate Wheel Drives. *IEEE Conference on Emerging Technologies and Factory Automation.*

[8] Hudha, K., Jamaluddin, H., Samin, P. M. and Rahman, R. A. (2003). Vehicle Modelling and Validations: Experience with Proton Car. *International Association of Vehicle System Dynamics (IAVSD).* August 24-30. Kanagawa, Japan.

[9] Samin, P.M., Jamaluddin H., Rahman, R. A, Anuar, S. and Hudha, K. (2008). Semi-Active Suspension System For Handling Quality and Longitudinal Stability Improvements Using Hybrid Stability Augmentation System-Force Control Algorithm. *2nd Regional Conference on Vehicle Engineering and Technology*. 15-16 July. Kuala Lumpur, Malaysia.

[10] Abu Bakar, S. A., Rahman, R. Abd., Jamaluddin, H., Rahman, Samin, P. M., Hudha, K., (2008) Vehicle Ride Performance With Semi Active Suspension System Using Modified Skyhook Control Algorithm and Current Generator Control. *International Journal Of Vehicle Autonomous System*. Vol. 6, No. 3, pp 197-121.

[11] Karnopp, D., Crosby, M. J. and Farwood R.A. (1974). Vibration Control Using Semi-active Force Generators. *ASME Journal Of Engineering Industry*. 96(2):619-626.

ACKNOWLEDGEMENT

The authors wish to acknowledge the supports given by the Tokai University, Japan and Universiti Teknologi Malaysia that has made this research successful.

Table 2 RMS values of the studied responses during pitch simulation test

	60:40WD	40:60WD	Semi Active (40:60WD)	Improvement (Over 60:40WD) %	Improvement (Over 40:60WD) %
Jerk	120.2	119.7	92.95	22.7	22.7
Acceleration	2.198	2.198	1.622	26.2	26.2
Displacement	0.01025	0.00998	0.005616	51.1	49.8
Pitch Rate	0.05008	0.04888	0.02836	49.4	48.2
Pitch Angle	0.007666	0.007793	0.00446	49.2	50.0
Average Improvement (%)				39.7	39.3

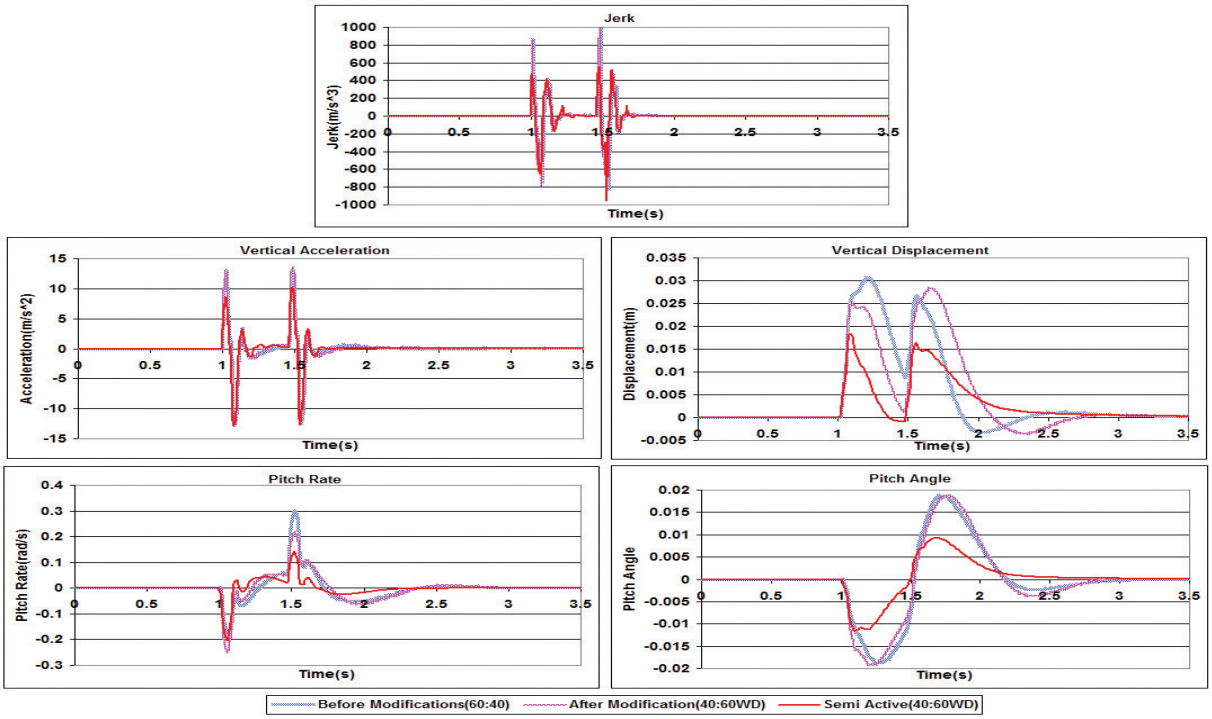

Fig. 9 Evaluations during pitch simulation test

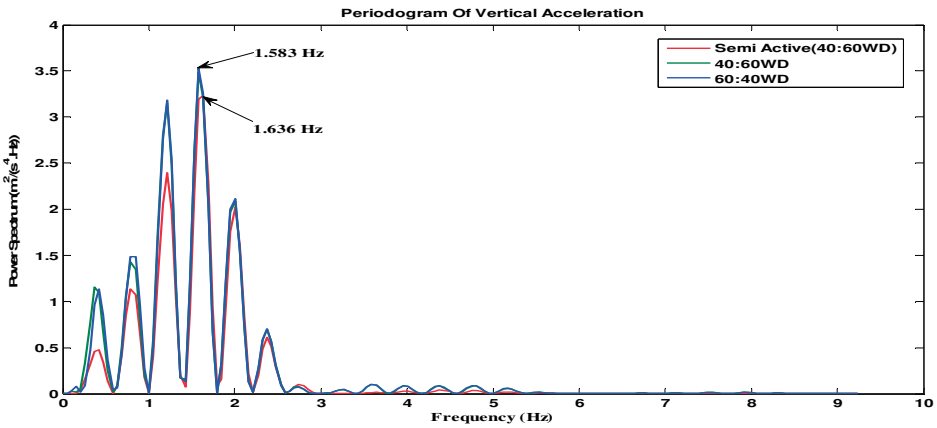

Fig. 10 Frequency domain analysis of EV conversion

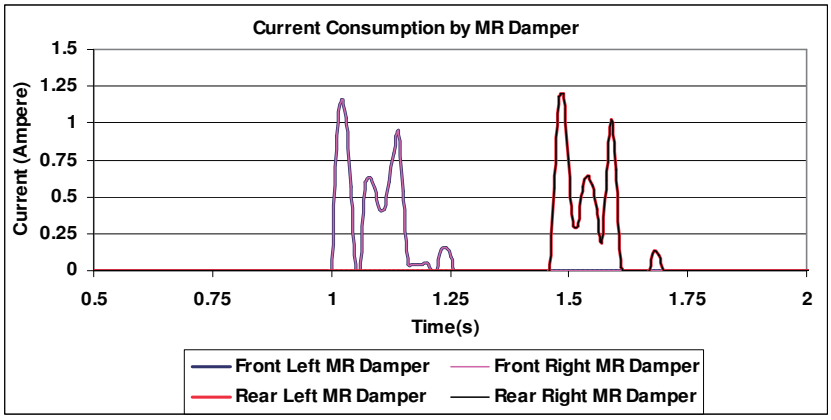

Fig. 11 MR damper current consumption

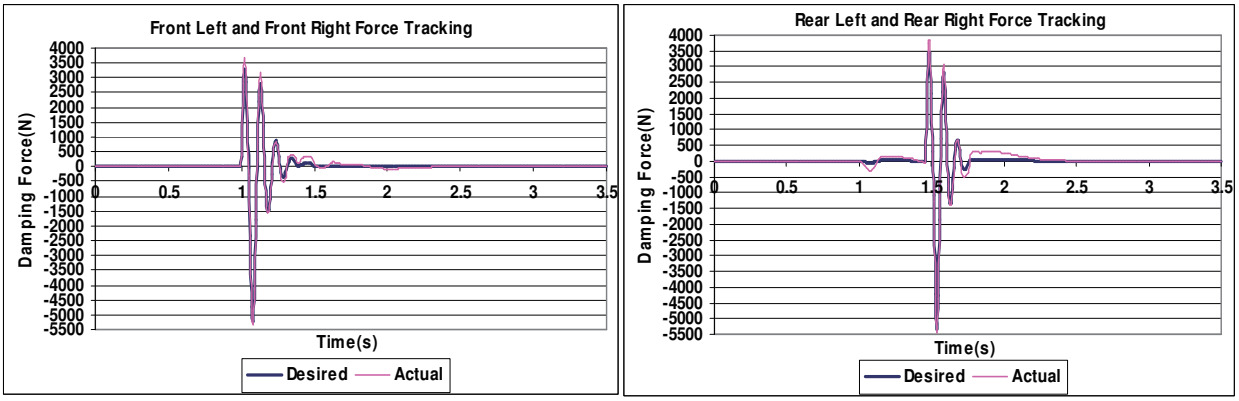

Fig. 12 Force tracking in magnetorheological semi active suspension system